

Tomasz Bednarski\*, Eryk Czerwiński, Paweł Moskal, Piotr Białas, Krzysztof Giergiel, Łukasz Kapton, Andrzej Kochanowski, Grzegorz Korcyl, Jakub Kowal, Paweł Kowalski, Tomasz Kozik, Wojciech Krzemień, Marcin Molenda, Ines Moskal, Szymon Niedźwiecki, Marek Pałka, Monika Pawlik, Lech Raczyński, Zbigniew Rudy, Piotr Salabura, Neha Gupta Sharma, Michał Silarski, Artur Słomski, Jerzy Smyrski, Adam Strzelecki, Konrad Jan Szymański, Wojciech Wiślicki, Piotr Witkowski, Marcin Zieliński and Natalia Zoń

# Calibration of photomultipliers gain used in the J-PET detector

**Abstract:** Photomultipliers are commonly used in commercial PET scanner as devices that convert light produced in scintillator by gamma quanta from positron-electron annihilation into electrical signal. For proper analysis of obtained electrical signal, a photomultiplier gain curve must be known, since gain can be significantly different even between photomultipliers of the same model. In this article, we describe single photoelectron method used for photomultiplier calibration applied for J-PET scanner, a novel PET detector being developed at Jagiellonian University. A description of calibration method, an example of calibration curve, and a gain of few Hamamatsu R4998 photomultipliers are presented.

**Keywords:** photomultiplier calibration; single photoelectron.

\*Corresponding author: **Tomasz Bednarski**, Institute of Physics, Jagiellonian University, 30-059 Kraków, Poland, E-mail: tomasz.bednarski@uj.edu.pl

**Eryk Czerwiński, Paweł Moskal, Piotr Białas, Krzysztof Giergiel, Grzegorz Korcyl, Jakub Kowal, Tomasz Kozik, Wojciech Krzemień, Ines Moskal, Szymon Niedźwiecki, Marek Pałka, Monika Pawlik, Zbigniew Rudy, Piotr Salabura, Neha Gupta Sharma, Michał Silarski, Artur Słomski, Jerzy Smyrski, Adam Strzelecki, Konrad Jan Szymański, Piotr Witkowski, Marcin Zieliński and Natalia Zoń:** Institute of Physics, Jagiellonian University, Kraków, Poland

**Łukasz Kapton:** Institute of Physics, Jagiellonian University, Kraków, Poland; and Faculty of Chemistry, Jagiellonian University, Kraków, Poland

**Andrzej Kochanowski and Marcin Molenda:** Faculty of Chemistry, Jagiellonian University, Kraków, Poland

**Paweł Kowalski, Lech Raczyński and Wojciech Wiślicki:** Świerk Computing Centre, National Centre for Nuclear Research, Otwock-Świerk, Poland

## Introduction

Positron emission tomography (PET) allows to imagine spatial distribution of injected substance and temporal changes of biological and chemical processes inside the body. It is used in medical diagnostics (e.g., oncology and cardiology) and to monitor changes in brain of people with mental diseases. Tomographs (which are currently commercially used) consist of hundreds of scintillating crystals that detect gamma radiation coming from decay of radioactive pharmaceuticals injected into the patient's bloodstream. Scintillating crystals are usually grouped in blocks with dimensions up to 5×5 cm. At the rear of each block, typically four photomultipliers convert light pulses into electrical signals. Reconstruction of images is mainly based on signals coming from the photoelectric effect in scintillating crystals [1].

Calibration check of PET device with radioactive source is done every day before patient examination to control if all photomultipliers are set to the same gain value. If needed, a change of applied voltage must be done according to individual calibration curve.

## Definition of photomultiplier tube (PMT) gain

A photon, which hits a photomultiplier's photocathode, can release a photoelectron. The emitted photoelectron is accelerated in an electric field inside photomultiplier. Thus, after striking the first dynode, secondary electron emissions occur. The secondary emissions are repeated over all dynodes resulting in a high current amplification (Figure 1). Secondary electron emission ratio  $\delta$  between two dynodes is given by  $\delta = A \cdot E^\alpha$ , where  $A$  is a constant,  $E$  is an interstage voltage, and  $\alpha$  is a coefficient depending

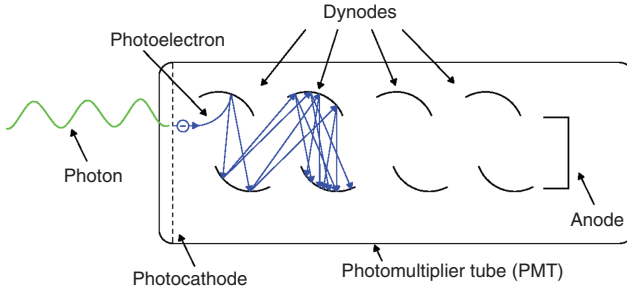


**Figure 1** A PMT scheme with secondary electron emissions.

on the dynodes and the geometric structure. In a photomultiplier with  $n$  dynodes, gain  $\mu$  becomes

$$\mu = \delta^n = (A \cdot E^\alpha)^n = K \cdot V^{cn}, \quad (1)$$

where  $K$  is a constant and  $V$  is a voltage applied between cathode and anode [2].

For a given amount of light reaching the photocathode at the applied voltage, the charge of produced electric signal is proportional to the gain of a given photomultiplier. However, gain of photomultipliers can be significantly different even for the same model of photomultiplier, as shown in Figure 2 (Hamamatsu R4998 photomultipliers [2] with 2250 V applied, optimal for the model).

Thus, for proper functionality of PET devices, photomultiplier gain calibration is important.

## Calibration of single PMT

One of the methods of determination of the calibration curve of PMT is to measure a charge of the PMT signal

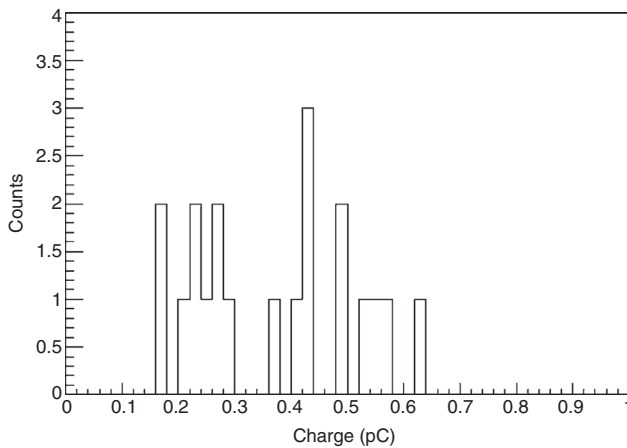


**Figure 2** Single photoelectron charge for 20 Hamamatsu R4998 photomultipliers with applied high voltage of 2250 V.

when a particular amount of light is directed on a photomultiplier's photocathode; therefore, pulse lasers are commonly used as the light sources. The other possibility is to monitor the light intensity of the source with a proper device (e.g., avalanche photodiode) [3]. A different approach is to measure charge from a PMT when only a single photon reacts with the photocathode. If light intensity is low, then it may happen that zero or only one of photons interacts with the photocathode-releasing photoelectron. To obtain the low intensity of light, the additional attenuation can be introduced [4]. A number of photoelectrons can be also estimated from observed signals produced by a radioactive source of known radiation energy when relation between number of released photoelectrons and energy of the observed signal is known [5].

In this article, we present a calibration method based on the single photoelectron approach used for J-PET at Jagiellonian University [6], with modifications mentioned in the next sections.

## Single photoelectron method

Gamma quanta going through the scintillating material can excite medium atoms (the scintillator used during the calibration was RP-422 produced by Rexion with light output of about 8400 photons per 1 MeV of deposited energy [7, 8]). During atom de-excitation, photons are isotropically emitted. Some of them may fly away from the scintillator, but others can be internally reflected and reach its end, where a photomultiplier is attached. Two methods can be applied in order to have reaction of only one photon with the PMT photocathode from a hit of a single gamma quantum in the scintillator: (i) the light output of the scintillator must be attenuated or (ii) an aperture between the photomultiplier and the scintillator is inserted to restrict area of the photocathode that can be hit by photons. The second method is in use for the J-PET project.

If we assume that the probability to produce a photoelectron in the photocathode is the same for each photon reaching the edge of the scintillator, then the probability distribution of the number of photoelectrons is given by the Bernoulli distribution:

$$P_k^{N_{\text{ph}}} = \binom{N_{\text{ph}}}{k} p^k (1-p)^{N_{\text{ph}}-k}, \quad (2)$$

where  $N_{\text{ph}}$  is the number of photons reaching the end of the scintillator,  $k$  is the number of photoelectrons released from the photocathode, and  $p$  is a probability that a photon

reaching the edge of the scintillator will cause emission of photoelectron. This probability can be defined as follows:

$$p = \varepsilon \cdot \frac{A_{\text{aperture}}}{A_{\text{scintillator}}}, \quad (3)$$

where  $A$  is area of an aperture ( $0.28 \text{ mm}^2$ ) and a scintillator cross-section ( $196 \text{ mm}^2$ ) and  $\varepsilon$  is cathode quantum efficiency (which is about 20% for used Hamamatsu R4998 PMT model [2]). For the above-mentioned values,  $p = 2.88 \cdot 10^{-4}$ . Based on Eq. (2), probability for 0, 1, and 2 photoelectrons can be written as

$$P_0^{N_{\text{ph}}} = (1-p)^{N_{\text{ph}}}, \quad (4)$$

$$P_1^{N_{\text{ph}}} = N_{\text{ph}} \cdot p \cdot (1-p)^{N_{\text{ph}}-1}, \quad (5)$$

$$P_2^{N_{\text{ph}}} = \frac{1}{2} N_{\text{ph}} \cdot (N_{\text{ph}} - 1) \cdot p^2 \cdot (1-p)^{N_{\text{ph}}-2}. \quad (6)$$

Based on Eqs. (4) to (6), the ratio between number of events with 0, 1, and 2 photoelectrons can be calculated as

$$\frac{N_0}{N_1} = \frac{1-p}{N_{\text{ph}} \cdot p}, \quad (7)$$

$$\frac{N_1}{N_2} = \frac{2(1-p)}{(N_{\text{ph}} - 1) \cdot p}. \quad (8)$$

Dependence of ratios from Eqs. (7) and (8) on probability  $p$  is shown in Figure 3.

The number of photons used to obtain ratios in Figure 3 was derived from the average signal charge spectrum from the reference photomultiplier (mentioned in

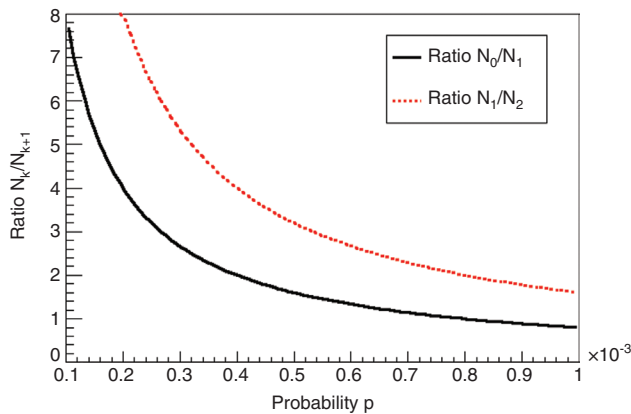


**Figure 3** Calculated ratios of consecutive number of observed photoelectrons as a function of probability of releasing photoelectron from a photocathode.

the next section) and is  $N_{\text{ph}} = 1250$ . From Figure 3, we can infer that ratio of number of events with 1 and 2 photoelectrons should be about two times larger than for ratio of events with 0 and 1 photoelectron.

## Measurement setup and data collection

The measurement setup consists of two Hamamatsu R4998 photomultipliers [2], a Rexion scintillator RP422 [7] with dimensions of  $14 \times 14 \times 100 \text{ mm}^3$ , a  $^{22}\text{Na}$  radioactive source, and a LeCroy WaveRunner 64Xi oscilloscope [9]. Between the scintillator and the tested photomultiplier, an aperture with a hole diameter of 0.6 mm was inserted (Figure 4).

The second photomultiplier was used as a reference detector, while the oscilloscope was used to collect the complete shape of each signal. Signals from the calibrated photomultiplier were collected only when the reference PMT gave a signal in order to avoid collecting a photomultiplier thermal noise. A distribution of signals charge from the calibrated photomultiplier is shown in Figure 5.

In the distribution in Figure 5, one can distinguish three maxima. From the left side: a maximum from events when no photoelectron was released from a photocathode, a maximum from a one photoelectron, and a maximum from two photoelectrons. The two photoelectrons maximum shows up as a bump on the right side of the one photoelectron maximum. Fitted curve  $F$  is a sum of three Gaussian functions given as

$$F = N_0 \cdot \exp\left(\frac{-(x - X_0^0)^2}{2\sigma_0^2}\right) + N_1 \cdot \exp\left(\frac{-(x - X_1^0)^2}{2\sigma_1^2}\right) + N_2 \cdot \exp\left(\frac{-(x - X_2^0)^2}{2\sigma_2^2}\right), \quad (9)$$

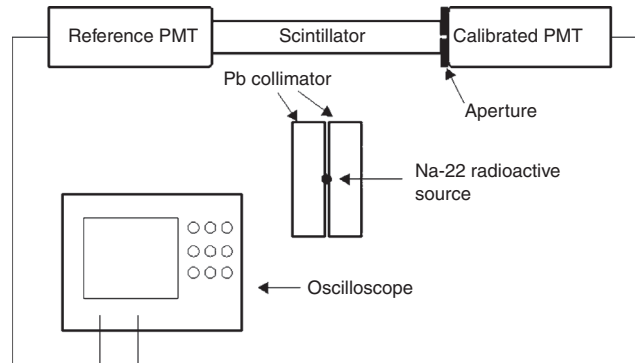


**Figure 4** A scheme of measurement setup.

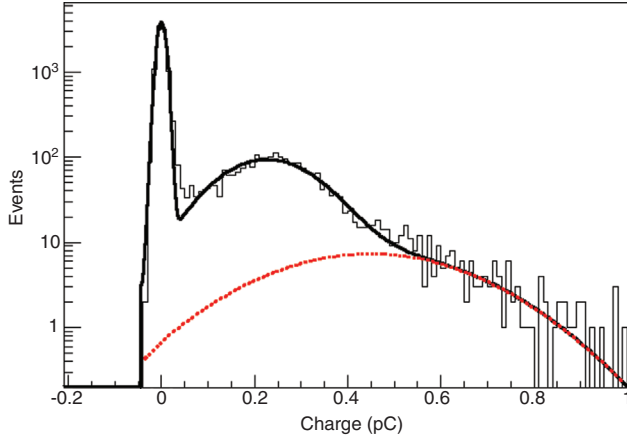


**Figure 5** A histogram of charge distribution collected during the measurement. Fitted curve is a sum of three Gaussian functions. From the left side: around 0 pC, a case when no photoelectron was emitted and single (around 0.25 pC) and two (around 0.5 pC) photoelectrons maximum. The red dashed line is separately drawn for two photoelectrons maximum.

where  $N_x$ ,  $X_x^0$ ,  $\sigma_x$  ( $x=0,1,2$ ) correspond to normalizations, center of maxima, and standard deviations, respectively.

Because the gathered charge should scale linearly with the number of observed photoelectrons, the position of the center of two photoelectrons maximum is, as expected, two times larger than for one photoelectron. Therefore, in order to decrease the number of fitted parameters, Eq. (9) can be rewritten as

$$F = N_0 \cdot \exp\left(\frac{-(x - X_0^0)^2}{2\sigma_0^2}\right) + N_1 \cdot \exp\left(\frac{-(x - X_1^0)^2}{2\sigma_1^2}\right) + N_2 \cdot \exp\left(\frac{-(x - 2X_1^0)^2}{2\sigma_2^2}\right). \quad (10)$$

Values of fitted parameters allow for the determination of ratios from Eqs. (7) and (8). To compare the experimental results with the predictions, one can use Eq. (8) to perform an estimation of  $N_{\text{ph}}$ . For ratio obtained from Figure 5, ( $N_1/N_2=6.89$ ) and the known value of  $p=2.88 \cdot 10^{-4}$ , one obtains  $N_{\text{ph}}=1139$  photons, which is in good agreement with the value derived from the reference detector  $N_{\text{ph}}=1250$ .

## Calibration curve

The information about charge induced in a photomultiplier from a single photoelectron allows for the determination of a PMT gain curve. The gain changes with the voltage applied on the PMT (Eq. (1)). Therefore, measurement of

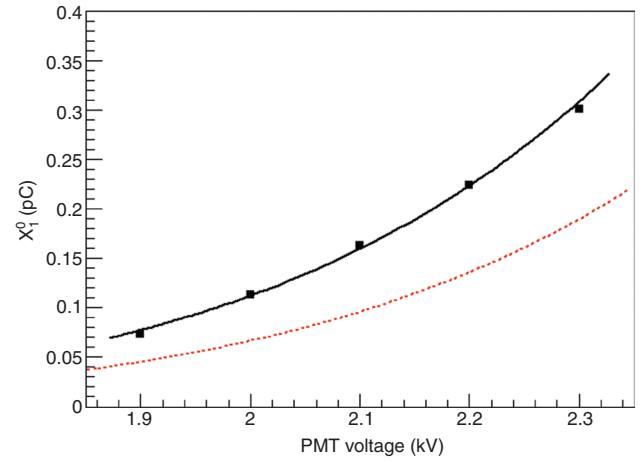


**Figure 6** A power function (black solid line) of form  $A \cdot x^B$  fitted to experimental data points. Derived parameters:  $A=(7.31 \pm 0.43) \cdot 10^{-4} [\text{pC}/\text{kV}^B]$  and  $B=7.252 \pm 0.098$ . The experimental errors are smaller than presented data points. For comparison, gain curve (red dashed line) for the other photomultiplier is shown.

the charge given by the PMT for the single photoelectron event as a function of voltage applied to it allows for the determination of the gain curve. An example of such curve is shown in Figure 6. The curve (black solid line) of a form given in Eq. (1) is fitted to the experimental data points.

In Figure 6, additional gain curve (for other photomultiplier) is shown as red dashed line. To set the same value of gain (charge induced for single photoelectron about  $0.16 \text{ pC} = 10^4 \text{ e}$ ) on both photomultipliers, voltage of about 2100 and 2250 V has to be applied on first and second ones, respectively.

## Summary

The single photoelectron method was described, which enables to determine the gain curve for photomultiplier needed for calculation of a number of photoelectrons in observed signal. The number of photoelectrons is more convenient to use in comparison of signals instead of signal charge, since it does not depend on voltage applied to the photomultiplier.

Gain of photomultipliers can differ significantly even for the same model. Therefore, gain calibration is necessary for proper operation of PET devices.

**Acknowledgments:** We acknowledge the technical and administrative support by M. Adamczyk, T. Gucwa-Ryś, A. Heczko, M. Kajetanowicz, G. Konopka-Cupiał, J. Majewski, W. Migdał, and A. Misiak and the financial support by the

Polish National Center for Development and Research through grant INNOTECH-K1/IN1/64/159174/NCBR/12, the Foundation for Polish Science through MPD program, the EU and MSHE Grant No. POIG.02.03.00-161 00-013/09, and the Małopolskie Centre of Entrepreneurship through Doc-tus program.

### Conflict of interest statement

**Authors' conflict of interest disclosure:** The authors stated that there are no conflicts of interest regarding the

publication of this article. Research funding played no role in the study design; in the collection, analysis, and interpretation of data; in the writing of the report; or in the decision to submit the report for publication.

**Research funding:** None declared.

**Employment or leadership:** None declared.

**Honorarium:** None declared.

Received October 29, 2013; accepted January 7, 2014; previously published online February 15, 2014

## References

1. Saha GB. Basics of PET imaging, 2nd ed. New York: Springer, 2010:57.
2. Website: Hamamatsu. Photomultiplier tubes and assemblies for scintillation counting & high energy physics. Available at: [http://www.hamamatsu.com/resources/pdf/etd/High\\_energy\\_PMT\\_TPM0007E03.pdf](http://www.hamamatsu.com/resources/pdf/etd/High_energy_PMT_TPM0007E03.pdf). Accessed: 22 Oct 2013.
3. Abe K, Hayato Y, Iida T, Iyogi K, Kameda J, Kishimoto Y, et al. Calibration of the super-Kamiokande detector. arXiv:1307.0162 [physics.ins-det].
4. Ronzhin A, Albrow MG, Demarteau M, Los S, Malik S, Pronko A, et al. Development of a 10 ps level time of flight system in the fermilab test beam facility. Nucl Instrum Methods Phys Res A 2010;623:931–41.
5. Baturin V, Burkert V, Kim W, Majewsky S, Nekrasov D, Park K, et al. Time resolution of Burle 85001 micro-channel plate photomultipliers in comparison with Hamamatsu R2083. Nucl Instrum Methods Phys Res A 2006;562:327–37.
6. Moskal P, Bednarski T, Białas P, Ciszewska M, Czerwiński M, Heczko A, et al. TOF-PET detector concept based on organic scintillators. Nucl Med Rev 2012;15:(Suppl):C81.
7. Website: REXON. Plastic Scintillation Info. Available at: <http://www.rexon.com/plasticsinfo.htm>. Accessed: 22 Oct 2013.
8. Website: Eljen Technology. EJ-232. Available at: <http://www.eljentechnology.com/index.php/products/plastic-scintillators/68-ej-232>. Accessed: 22 Oct 2013.
9. Website: Teledyne Lecroy. Available at: <http://teledynelecroy.com/oscilloscope/oscilloscopemodel.aspx?modelid=1939&capid=102&mid=504>. Accessed: 22 Oct 2013.